Journal of Solid State Chemistry **148,** 150–157 (1999)
Article ID jssc.1999.8418, available online at http://www.idealibrary.com on IDEAL®

Hydrothermal Synthesis, Structure, and Magnetic Characterization of a New Ferrimagnetic Open Framework Phosphate: MIL-21 or $[Fe^{III}_{5-x}V^{III}_{x}(H_2PO_4)_4(HPO_4)_4F_4(H_2O)_2, 4(H_{2+y}N–(CH_2)_2–NH_{2+y})]$ with a Partial Cationic Disorder

Myriam Riou-Cavellec, Jean-Marc Grenèche,* and Gérard Férey[1]

*Institut Lavoisier, UMR CNRS 8637, 45 Avenue des Etats-Unis, 78035 Versailles Cedex, France; and *Laboratoire de Physique de l'Etat Condensé, Upresa CNRS 6087, Université du Maine, Avenue Olivier Messiaen, 72085 Le Mans Cedex 9, France*

Received February 2, 1999; in revised form June 4, 1999; accepted June 8, 1999

DEDICATED TO PROFESSOR C. N. R. RAO ON THE OCCASION OF HIS 65TH BIRTHDAY

MIL-21 or $[Fe^{III}_{5-x}V^{III}_{x}(H_2PO_4)_4(HPO_4)_4F_4(H_2O)_2, 4(H_{2+y}N–(CH_2)_2–NH_{2+y})]$ was prepared hydrothermally (453 K, autogenous pressure, 3 days) in the presence of ethylenediamine. Its structure was determined by single-crystal X-ray diffraction. MIL-21 is tetragonal (space group $P\text{-}42_1c$, No. 114, with cell parameters $a = 17.2023(2)$ Å, $c = 13.3086(2)$ Å, $V = 3938.27(9)$ Å^3, $Z = 4$. Its three-dimensional network can be described from the connection via phosphate tetrahedra of infinite corner-sharing *cis–trans* octahedral chains of metallic atoms in a random distribution and isolated $FeO_4(H_2O)_2$ octahedra. The (Fe^{3+}, V^{3+}) infinite chains belong to the KTP type. Mössbauer and structure refinements demonstrate this segregation. This structure exhibits small tunnels and cages in which the ethylenediamine molecules are located. Moreover, MIL-21 shows a ferrimagnetic behavior below 13 K.

INTRODUCTION

In addition to molecular sieve properties, open-framework iron phosphates have the potential to display either ferrimagnetic or antiferromagnetic properties. In 1994, the open-framework iron phosphate ULM-12 (1), which exhibits an antiferromagnetic ordering temperature at 11 K, was the first magnetic open framework iron phosphate to be synthesized hydrothermally with a templating organic species. Since then, a few iron phosphates (2–7) or fluorophosphates have been discovered. Among the latter (first labeled ULM-*n* then MIL-*n* (since 1997 for Materials of Institut Lavoisier)), ULM-3 (4), ULM-4 (5), ULM-12 (1, 6), ULM-15 (7), and ULM-19 (8) show 3-D open-framework structures. Unfortunately, all of them are antiferromagnets.

By incorporating two appropriate transition metal cations, we aimed to synthesize ferromagnetic or ferrimagnetic open-framework bimetallic materials in order to add magnetic selectivity to shape and size differentiation. Such a material might be used, for example, to separate paramagnetic gas molecules from diamagnetic ones. Currently, several bimetallic phosphates are referenced in the literature (9–13), but no mention of interesting magnetic properties appears.

According to the possibility of ferromagnetic coupling between Fe^{3+} and V^{3+} ions, this paper deals with the hydrothermal synthesis, the crystal structure, the characterization of the extent of cationic disorder, and the magnetic properties of the title compound determined by magnetization, susceptibility, and Mössbauer measurements.

EXPERIMENTAL

1. Synthesis

MIL-21 or $[Fe^{III}_{5-x}V^{III}_{x}(H_2PO_4)_4(HPO_4)_4F_4(H_2O)_2, 4(H_{2+y}N–(CH_2)_2–NH_{2+y})]$ ($x = 5/3$; $y = 1/8$) was prepared hydrothermally under autogenous pressure (453 K for 3 days). The reactive mixture was obtained by successively adding Fe_2O_3 (Aldrich, 99%+), VCl_3 (Aldrich), H_3PO_4 (Prolabo, 85%), HF (Prolabo, 48%), ethylenediamine (Aldrich, 99%+), and water in the molar ratios 1:2:4:2:4:80. The mixture was placed without stirring in a 23-ml Teflon vessel of a Parr acid digestion autoclave. The pH remained neutral from the initial stage to the end of the reaction. The resulting inhomogenous product was filtered off, washed with distilled water, and dried at room temperature. Few dark orange parallelepipedic crystals of medium optical quality were isolated from the bulk.

[1] To whom correspondence should be addressed.

0022-4596/99 $30.00

2. Physical Methods

Chemical analysis (wt%) of the sample indicated that V = 6.47% and Fe = 12.45%.

Energy dispersive X-ray spectrometry was also performed on the title compound using a Jeol SM-5800LV scanning microscope equipped with a Oxford Instruments microanalysis system (Link Isis). Several semiquantitative EDX results, realized in low vaccum, were in agreement with the chemical analysis and indicated an Fe/V atomic ratio close to 2. They also confirmed the presence of fluorine in the compound.

TGA measurements were performed under O_2 atmosphere using a TA-Instrument model 2050 analyzer. The heating rate was 5°C/min from 30 to 600°C. The TGA curve indicates a continuous weight loss of about 20% occurring in the 150–500°C temperature range. This corresponds to the departure of coordinated water molecules and of the four ethylenediamine molecules: $\%_{exp} \approx 20$; $\%_{theo} = 19.8$, which is in good agreement with the proposed formula of MIL-21. The amine loss leads to the collapse of the structure; the resulting product is amorphous.

TABLE 1
Crystal Data and Structure Refinement for MIL-21

$[Fe_{5-x}V_x(H_2PO_4)_4(HPO_4)_4F_4(H_2O)_2, 4(H_{2+y}N\text{–}(CH_2)_2\text{–}NH_{2+y})]$	
Wavelength	0.71073 Å
Crystal system	tetragonal
Space group	$P\text{-}42_1c$ (No. 114)
Unit cell dimensions	$a = 17.2023(2)$ Å
	$b = 17.2023(2)$ Å
	$c = 13.3086(2)$ Å
Volume, Z	3938.27(9) Å^3, 4
Density (calculated)	2.36 g/cm^3
Absorption coefficient	21.14 cm^{-1}
$F(000)$	2824
Theta range for data collection	1.67 to 31.15°
Limiting indices	$-16 \le h \le 24$, $-24 \le k \le 22$, $-18 \le l \le 19$
Reflections collected	59266
Independent reflections	5945 [R(int) = 0.0731]
Refinement method on F^2	Full-matrix least-squares
Data/restraints/parameters	5934/0/291
Final R indices [$I > 2\sigma(I)$]	$R_1 = 0.0655$, $wR_2 = 0.1375$
R indices (all data)	$R_1 = 0.0810$, $wR_2 = 0.1605$
Extinction coefficient	0.0016(2)
Largest diff. peak and hole	1.031 and −1.810 e Å^{-3}

3. Single Crystal Structure Determination

A single crystal with a limit quality for X-ray determination was isolated for data collection on a Siemens three-circle diffractometer equipped with a CCD bidimensional detector. Conditions of data measurements are summarized in Table 1. An absorption correction specific to the CCD detector was applied to all data using the SADABS program. From the collected data and the intensities of reflections, only the non centrosymetric space group $P\text{-}42_1c$ (No. 114) was possible.

The structure of $[Fe^{III}_{5-x}V^{III}_x(H_2PO_4)_4(HPO_4)_4F_4(H_2O)_2, 4(H_{2+y}N\text{–}(CH_2)_2\text{–}NH_{2+y})]$ was solved by direct methods using the TREF option of the SHELXTL crystallographic software package (14). The heaviest atoms (Fe, P) were first located on eight different crystallographic sites. The positions of remaining atoms (oxygen, fluorine, and organic elements) were deduced from Fourier difference calculations. Bond valence calculations and thermal factor considerations confirm the attribution of fluorine sites. There are two types of amines, labeled A and B in Tables 2 and 3. Geometrical constraints were applied to locate hydrogen atoms of diamine A. All the atomic positions were refined with an individual anisotropic thermal motion except H atoms for which an overall isotropic factor was applied. The thermal factors of nitrogen and carbon atoms of diamine B being quite high, it was not reasonable to try to locate hydrogen atoms on the latter; even N–C and C–C bond lengths are not too good.

In order to respect the chemical analysis results (Fe/V ratio ≈ 2), the structure refinement applied first Fe^{3+}–V^{3+} statistical occupancy on the four (fully occupied) metallic crystallographic sites (8*e*1, 8*e*2, 2*a*, and 2*b* sites of the $P\text{-}42_1c$ space group). With such a hypothesis, the refined Fe and V contents did not match with the chemical results and the reliability factors were worse than if Fe^{3+} is the only species in the octahedra. After the Mössbauer study, and in agreement with its results, the best fit is obtained when Fe^{3+} ions alone occupy the 2*a* and 2*b* sites while the two 8*e* sites contain both Fe^{3+} and V^{3+} in statistical occupancy, but with slightly different iron contents on the two sites *M*(3) and *M*(4) (see Table 2). This fact agrees with the Mössbauer data at 40 mK, where two distinguishable contributions of the 8*e* sites are clearly visible (see below). The examination of the structure and bond valence calculations (15) clearly indicate the existence of (HPO_4) and (H_2PO_4) groups; moreover, the charge equilibrium deduced from the existence of the hydrogenophosphate groups implies that the majority of the ethylenediamine molecules are neutral or monoprotonated for 25% of them, which is in agreement with the neutral pH observed during the synthesis. This led us to propose the following chemical formula for MIL-21: $[Fe^{III}_{5-x}V^{III}_x(H_2PO_4)_4(HPO_4)_4F_4(H_2O)_2, 4(H_{2+y}N\text{–}(CH_2)_2\text{–}NH_{2+y})]$ with x close to 5/3 to respect the initial Fe/V ratio established by chemical analysis, and $y = 1/8$. At the end of refinement cycles, reliability factors are quite high $R_1(F_o) = 6.55\%$, $wR_2(F_o^2) = 13.75\%$, but this can be easily explained by a limit quality of the collected crystal and also by the observed cationic disorder confirmed by Mössbauer data.

TABLE 2
Atomic Coordinates ($\times 10^4$, except for H Atoms $\times 10^3$), Occupancy Rates on Metallic Sites and Equivalent Isotropic Displacement Parameters ($Å^3 \times 10^3$)

	x	*y*	*z*	*U*(eq)	$\%Fe^{3+}$
M(1)	5000	5000	0	14(1)	100
M(2)	0	0	0	15(1)	100
M(3)	8179(1)	1932(1)	2492(1)	15(1)	59(2)
M(4)	7531(1)	2540(1)	9993(1)	15(1)	54(2)
P(1)	6742(1)	4196(1)	−488(1)	14(1)	
P(2)	9082(1)	3232(1)	1151(2)	17(1)	
P(3)	6044(1)	1833(1)	−1238(2)	17(1)	
P(4)	8343(1)	920(1)	494(1)	13(1)	
F(1)	7422(3)	2306(3)	1462(3)	18(1)	
F(2)	7762(3)	2644(3)	3531(3)	19(1)	
O(1W)	5000	5000	1431(6)	10(1)	
O(2W)	0	0	1445(5)	10(1)	
O(3)	6988(4)	3533(3)	191(4)	21(1)	
O(4)	6132(3)	4679(3)	38(4)	16(1)	
O(5)	8914(3)	415(3)	−69(4)	20(1)	
O(6)	6523(3)	1996(3)	−312(4)	22(1)	
O(7)	8642(3)	1228(3)	1490(4)	19(1)	
O(8)	6141(3)	2419(3)	−2078(4)	20(1)	
O(9)	7628(3)	389(4)	789(5)	27(1)	
O(10)	6499(3)	3936(3)	−1537(4)	18(1)	
O(11)	8870(4)	2802(5)	2092(5)	39(2)	
O(12)	5185(4)	1793(5)	−932(5)	34(2)	
O(13)	8052(4)	1550(3)	−211(4)	23(1)	
O(14)	6282(4)	1028(4)	−1701(5)	32(2)	
O(15)	7475(3)	4740(4)	−692(5)	24(1)	
O(16)	8549(3)	3072(4)	256(4)	25(1)	
O(17)	9102(6)	4104(4)	1394(9)	77(4)	
O(18)	9915(4)	3031(5)	866(5)	45(2)	
N(1A)	6464(4)	5301(4)	−2813(5)	24(1)	
N(2A)	6468(4)	4788(4)	2212(5)	27(2)	
C(1A)	6073(4)	3391(4)	2341(7)	27(2)	
C(2A)	6674(4)	4003(4)	2613(7)	26(2)	
N(1B)	6085(7)	858(10)	−3738(9)	65(4)	
N(2B)	9063(8)	4099(9)	−1307(10)	78(4)	
C(1B)	8969(15)	4655(19)	3394(13)	176(15)	
C(2B)	5797(16)	529(22)	1002(23)	227(23)	
H(1A)	648(4)	535(1)	−348(1)	44(8)	
H(2A)	600(1)	513(2)	−262(4)	44(8)	
H(3A)	683(2)	497(1)	−262(4)	44(8)	
H(4A)	686(2)	511(1)	231(4)	44(8)	
H(5A)	605(2)	497(2)	253(3)	44(8)	
H(6A)	637(4)	475(1)	156(1)	44(8)	
H(7A)	601(1)	338(1)	162(1)	44(8)	
H(8A)	626(1)	288(1)	255(1)	44(8)	
H(9A)	672(1)	403(1)	334(1)	44(8)	
H(10A)	717(1)	385(1)	235(1)	44(8)	

The atomic coordinates, the principal bond lengths are given in Tables 2 and 3. Values of both complete lengths and angles can be obtained on request to the authors.

4. Magnetic Measurements and ^{57}Fe Mössbauer Spectrometry

The magnetisation (*M*) of MIL-21 was measured as a function of the applied field *H* at many temperatures in the range 1.75 to 300 K with a Quantum Design Squid device. The resulting magnetic susceptibility χ was deduced. We

TABLE 3
Principal Bond Lengths [Å] in MIL-21

Fe(1)–O(1) w:	1.903(7)	⟨Fe(1)–O⟩ = 1.984(5)
Fe(1)–O(1) w:	1.903(7)	
Fe(1)–O(4):	2.024(5)	
Fe(1)–O(4):	2.024(5)	
Fe(1)–O(4):	2.024(5)	
Fe(1)–O(4):	2.024(5)	
Fe(2)–O(2) w:	1.923(7)	⟨Fe(2)–O⟩ = 1.976(5)
Fe(2)–O(2) w:	1.923(7)	
Fe(2)–O(5):	2.003(5)	
Fe(2)–O(5):	2.003(5)	
Fe(2)–O(5):	2.003(5)	
Fe(2)–O(5):	2.003(5)	
Fe(3)–O(8):	1.970(5)	⟨Fe(3)–O⟩ = 1.977(5)
Fe(3)–O(7):	1.972(5)	⟨Fe(3)–F⟩ = 1.989(4)
Fe(3)–O(10):	1.982(4)	
Fe(3)–F(2):	1.981(5)	
Fe(3)–O(11):	1.984(6)	
Fe(3)–F(1):	1.997(4)	
Fe(4)–O(13):	1.944(5)	⟨Fe(4)–O⟩ = 1.982(5)
Fe(4)–O(3):	1.965(5)	⟨Fe(4)–F⟩ = 1.999(4)
Fe(4)–F(2):	1.993(4)	
Fe(4)–F(1):	2.005(4)	
Fe(4)–O(16):	2.008(5)	
Fe(4)–O(6):	2.010(5)	
P(1)–O(4):	1.511(5)	⟨P(1)–O⟩ = 1.536(5)
P(1)–O(3):	1.517(5)	
P(1)–O(10):	1.524(5)	
P(1)–O(15):	1.591(6)	
P(2)–O(11):	1.499(6)	⟨P(2)–O⟩ = 1.521(6)
P(2)–O(18):	1.520(6)	
P(2)–O(16):	1.529(5)	
P(2)–O(17):	1.536(7)	
P(3)–O(6):	1.510(5)	⟨P(3)–O⟩ = 1.532(5)
P(3)–O(8):	1.514(5)	
P(3)–O(12):	1.533(6)	
P(3)–O(14):	1.571(6)	
P(4)–O(5):	1.511(5)	⟨P(4)–O⟩ = 1.532(5)
P(4)–O(7):	1.517(5)	
P(4)–O(13):	1.518(6)	
P(4)–O(9):	1.583(6)	
N(1A)–C(1A):	1.49(1)	
C(1A)–C(2A):	1.52(1)	
C(2A)–N(2A):	1.50(1)	
N(1B)–C(2B):	1.03(5)	
C(2B)–C(1B):	1.75(4)	
C(1B)–N(2B):	1.12(3)	

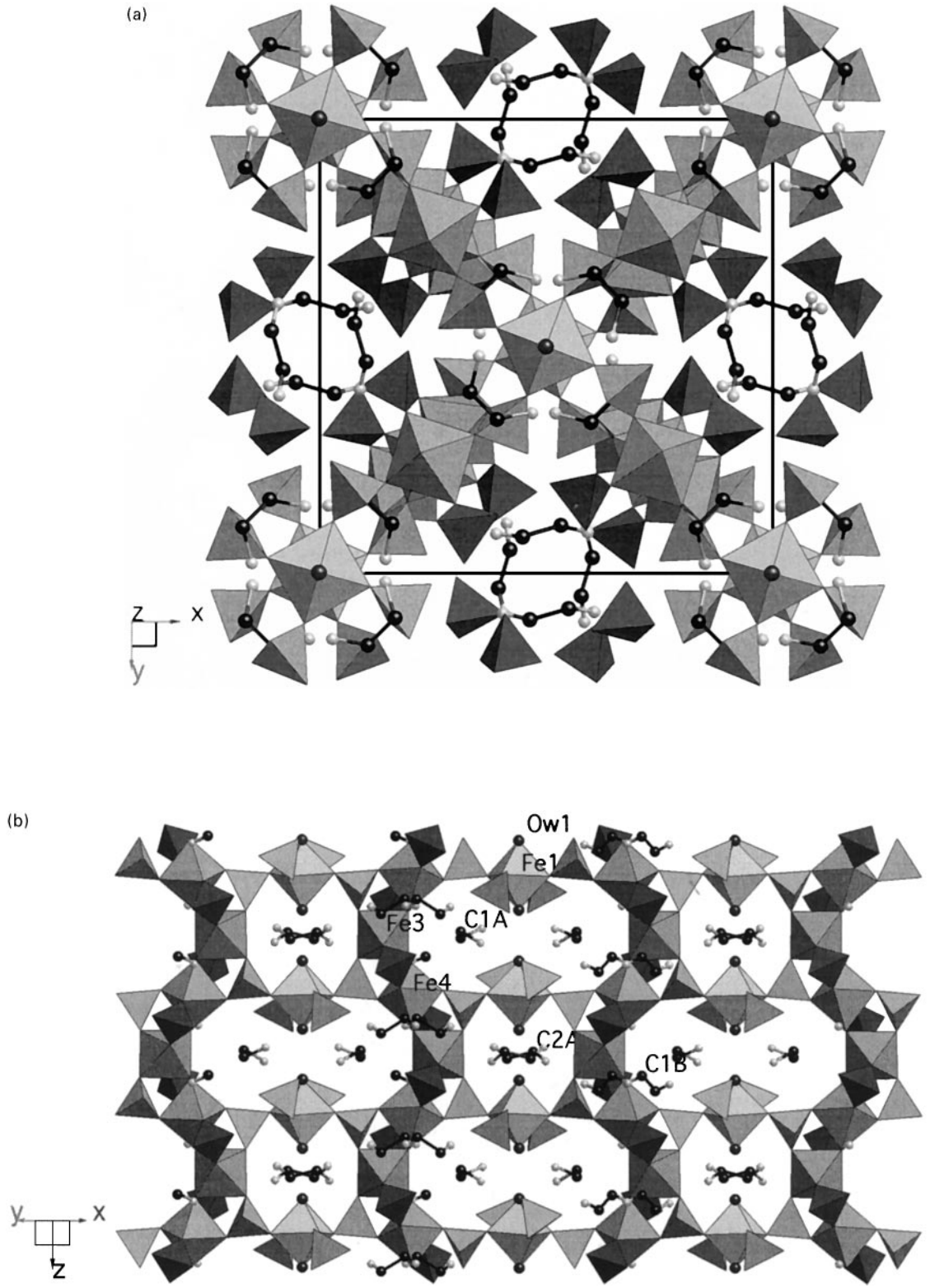

FIG. 1. (a) Projection of the 3-D structure of MIL-21 along the [001] direction. The isolated Fe^{3+} octahedra appear with their terminal water molecules (in black); the dihydrogenophosphates (black tetrahedra) of the $[H_xPO_4]^-$ grafted (Fe,V)(3, 4) chains (see text) create tunnels in which amines B are located, whereas the partially hidden amines A fill the cages limited by Fe(1, 2) isolated octahedra along [001]. (b) [110] Projection of MIL-21 which shows both the *cis–trans* chains along the *c* axis and the isolated octahedra, tunnels and "p-shaped orbital" cages.

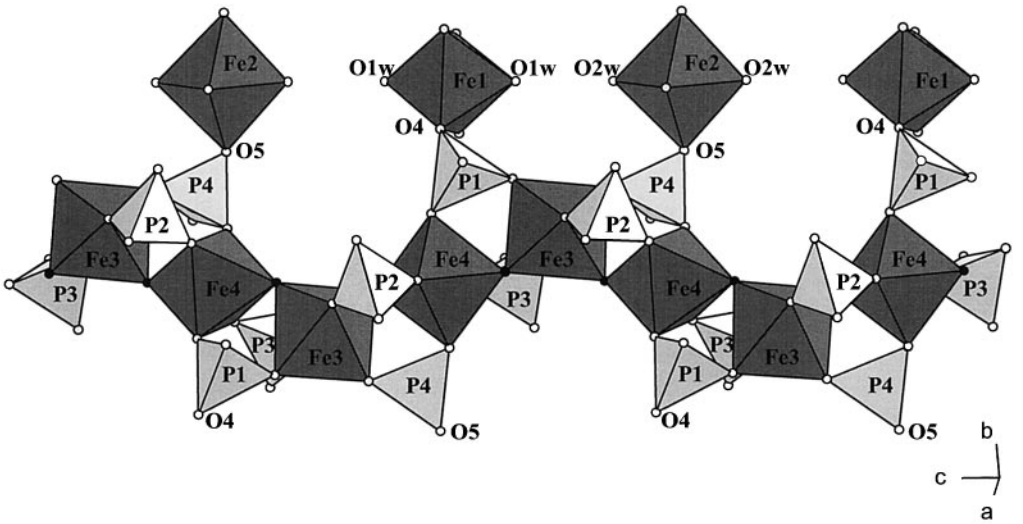

FIG. 2. Infinite chains with the KTP type for the octahedral sequence with labels corresponding to those in Table 2. Fluorine atoms are black spheres. The O(4) and O(5) oxygen atoms which ensure the three-dimensionality of the structure are indicated.

also measured the magnetization as a function of temperature varying the magnetic field.

Mössbauer experiments were carried out at 300, 77, and 4.2 K by means of a bath cryostat and at 40 mK with a dilution device system, using a constant acceleration spectrometer and a ^{57}Co source diffused into a Rh matrix. The values of the isomer shifts are quoted relative to α-Fe foil at 300 K. The hyperfine parameters were refined using a least-square fitting procedure in MOSFIT program (16).

RESULTS AND DISCUSSION

1. Description of the Structure

MIL-21 is three-dimensional and displays small "p-shaped orbital" cages and tunnels along [001] in which ethylenediamine molecules A and B are located, respectively (Figs. 1a and 1b). Within the inorganic framework, all the metallic cations Fe^{3+} and V^{3+} are sixfold coordinated. The Mössbauer study shows (see below) that metallic sites $M(1)$ and $M(2)$ correspond to $FeO_4(H_2O)_2$ isolated octahedra with terminal water molecules, whereas metallic sites $M(3)$ and $M(4)$ are occupied both by randomly distributed Fe^{3+} and V^{3+} and form $MO_{4/2}F_{2/2}$ infinite chains of octahedra along the c axis (Table 2, Fig. 1b).

The octahedra of these $MO_{4/2}F_{2/2}$ infinite chains (Fig. 2) are corner linked by fluorine atoms, each octahedron sharing two of its apices with two neighboring octahedra. The fluorine atoms are either in *trans* position or in *cis* position on the octahedra [$(Fe, V(4)F_2O_4)$ and $(Fe, V(3)F_2O_4)$, respectively]. This *cis–trans* connection was already encountered in KTP structure type (17, 18). A simple way for describing the whole structure considers that all the phosphate groups [$(HO)P(1,4)O_3$ and $(HO)_2P(2,3)O_2$] as well are grafted by two of their oxygen corners to the *cis–trans* chain. This topology implies that [$(HO)_2P(2,3)O_2$] groups belong to only one chain since their two last corners are (OH) moieties, whereas the last non-(OH) corner of [$(HO)P(1,4)O_3$] tetrahedra allows a sharing with Fe(1, 2) octahedra. The grafted infinite chain is close to that encountered in mineral tancoite or in ULM-14 (19). The main difference concerns the fluorine atoms which are always in *trans* position in the latter. Therefore, to ensure the framework, four different chains are related to each other via O(4) and O(5) atoms of the [$Fe(1,2)O_4(H_2O)_2$] isolated octahedra. This connection then delimits small "*p*-shaped

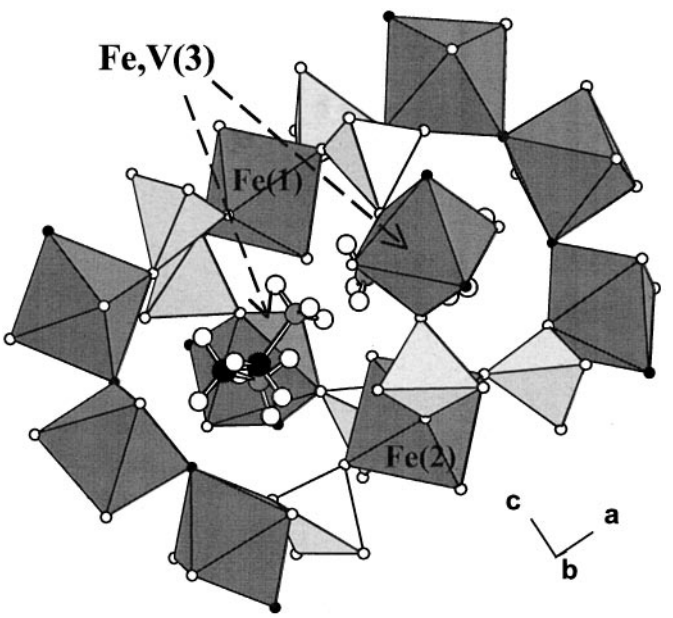

FIG. 3. Representation of a "p-shaped orbital" cage delimited by $M(3,4)$ chains and $M(1,2)$ octahedra.

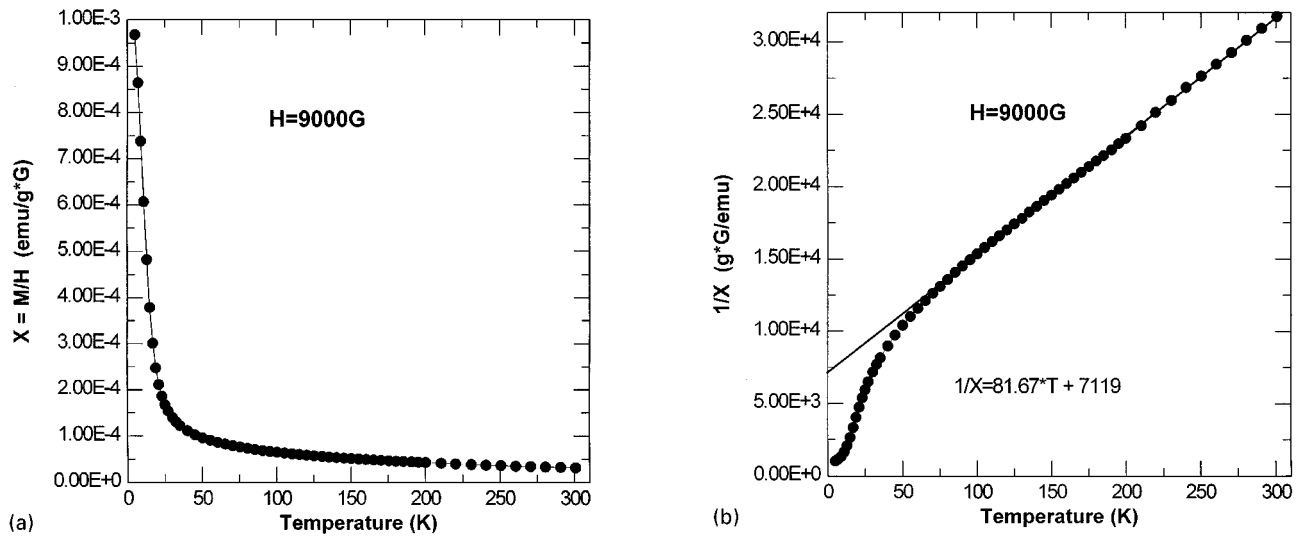

FIG. 4. (a) Variation of the magnetic susceptibility of MIL-21 as a function of temperature. (b) Thermal variation of the inverse magnetic susceptibility indicating a ferrimagnetic behavior under $T_C \approx 13$ K.

orbital" cages and tunnels along [001] (Fig. 1b). The small cages (Fig. 3) thus limited by four $M(3,4)$ chains and $M(1,2)$ octahedra are occupied by diamines A. Diamines B are located in the tunnels formed by eight H_2PO_4 tetrahedra.

2. *Magnetic Results and Discussion of the Degree of Cationic Order*

Figures 4a and 4b show the thermal evolution of the direct and inverse magnetic susceptibility, characteristic of a ferrimagnetic behavior below $T_C = 13$ (1) K. There is a good agreement between the calculated (16.25) and experimental (16.4 (3)) Curie constants related to five metallic atoms per formula unit (10/3 Fe^{3+} and 5/3 V^{3+}), the magnetization being expressed in Bohr magnetons. M(H) also indicates that the saturation is still not reached even at 1.75 K (Fig. 5).

The most significant spectra are given in Fig. 6. At 300 and 77 K (Fig. 6a), the observed quadrupolar doublets can be reproduced by at least two quadrupolar components in agreement with the presence of two main contributions of iron sites, i.e., (i) Fe(1) and Fe(2) in 2*a* and 2*b* and (ii) Fe(3) and Fe(4) in 8*e*1 and 8*e*2. The hyperfine characteristics (Table 4) indicate Fe^{3+} in a high spin state in octahedral units and are consistent with those previously observed in ULM-3 (4), ULM-12 (1), and ULM-14 (19) which also exhibit FeF_2O_4 octahedral units.

On the basis of both quadrupolar splitting values and relative absorption areas, one can assign the outer doublet to Fe(1) and Fe(2) sites (with SQ = 1.23 mm s^{-1}) and the inner doublet to Fe(3) and Fe(4) sites (with SQ = 0.46 mm s^{-1}). Indeed, in the case of ferric compounds, the larger the octahedral distortion (Δ), the higher the quadrupolar splitting (SQ). Applying Shannon's relationship (20) to the present system, the octahedral distortions of Fe(1), Fe(2), Fe(3), and Fe(4) sites are $10^4\Delta = 8.56$, 3.67, 0.20, and 1.53, respectively, and confirm the above assessment. Under such conditions, if there was an identical random distribution of Fe^{3+} and V^{3+} on the four sites, the proportions between the surfaces of the two kinds of doublets would be 1 : 4, but the refinement gives a ratio of 29/71 at 300 K and 37/63 at 77 K. Keeping in mind the content of the cell (20 metallic atoms) and the analytical (Fe/V = 2) ratio, that means that 40/3 Fe^{3+} ions must be distributed on the two types of sites. According to the above Mössbauer results, 29% of the whole content of iron(III) on the 2*a* and 2*b* sites correspond

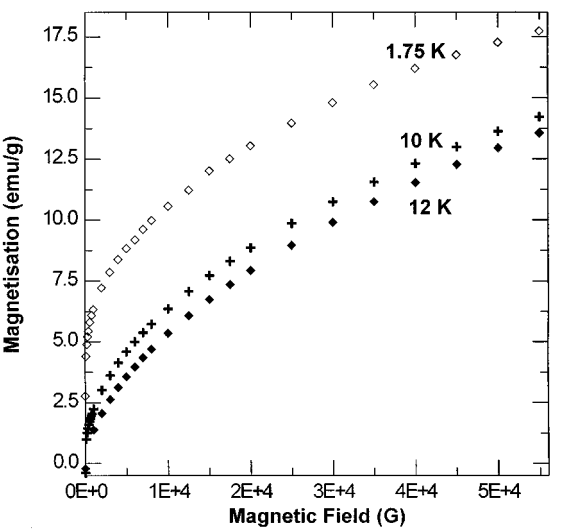

FIG. 5. M(H) curves at different temperatures below T_C. At 1.75 K, the saturation is not reached, even in high applied fields.

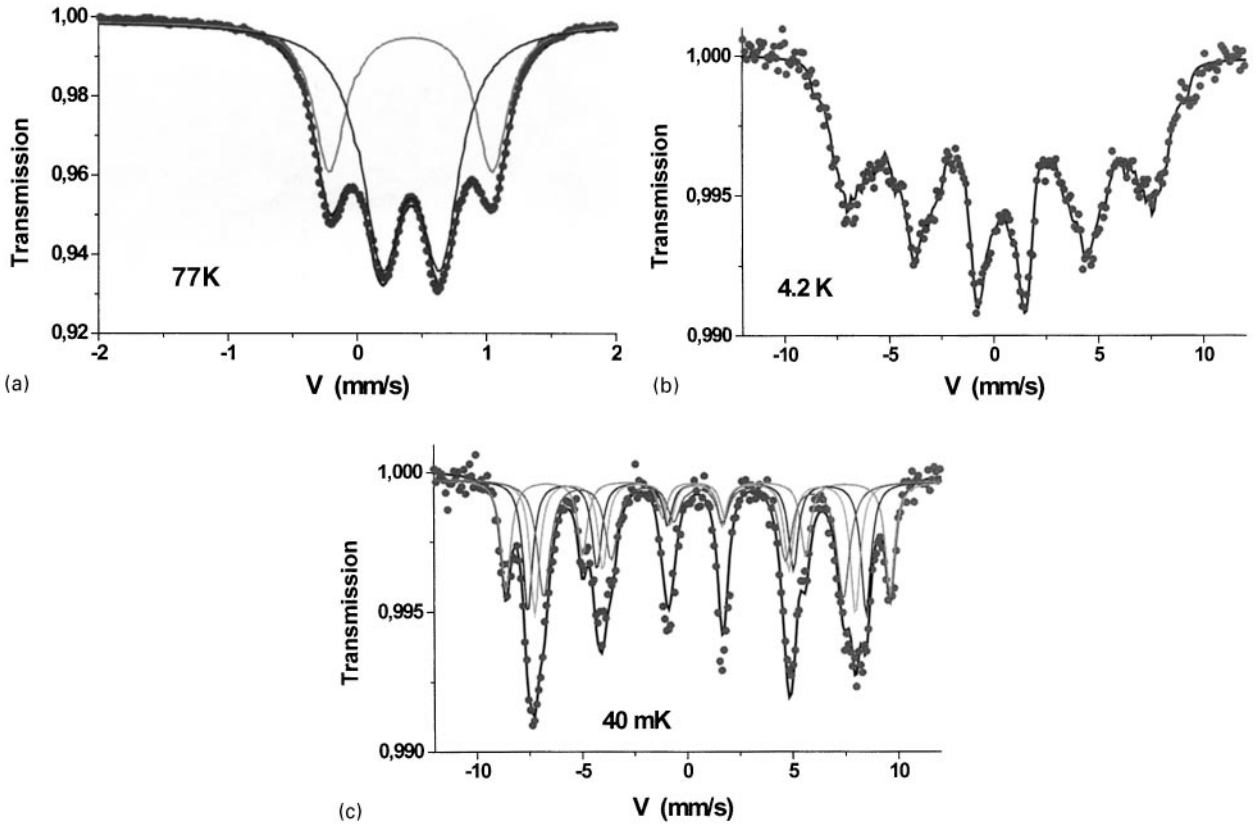

FIG. 6. Mössbauer spectra of MIL-21 recorded at 77 K (a), 4.2 K (b), and 40 mK (c).

to ca. 4 Fe^{3+} ions on these sites, which means with a good approximation their full occupancy by iron. As stated before, the refinement of the structure with these data gave the best fit. That means also that the two 8*e* sites contain 28/3 Fe^{3+} ions and 20/3 V^{3+} ions and then a 7 : 5 Fe^{3+}/V^{3+} ratio in the chains.

At 4.2 K (Fig. 6b), the unresolved lines are due to both the vicinity of T_C and the cationic disorder. When recorded at 40 mK, the spectrum (Fig. 6c) exhibits magnetic components with, however, broad lines, mainly on the inner sextet. Consequently, many fitting procedures can be applied involving different sets of magnetic sextets. The best fit obtained (Fig. 6c) involved four magnetic components, gathered in two groups according to the number of Fe sites. The hyperfine field of the narrow external sextet is then close to 56 T, whereas those of the broad internal sextet, with two distinguishable contributions, range from 43 to 50 T.

The assignement of the different measured hyperfine fields to special crystallographic sites requires to come back to the structure. It was shown that four different $[(Fe, V)(3,4)F_2O_4]$ octahedral chains are linked via $[HP(1,4)O_4]$ tetrahedra to $[Fe(1,2)O_4(H_2O)_2]$ isolated octahedra. That implies two types of magnetic interactions: superexchange through F^- ions between $(Fe, V)(3)^{3+}$ and $(Fe, V)(4)^{3+}$ ions within the chain, and supersuperexchange coupling through $[HP(1,4)O_4]$ tetrahedra between $Fe(1,2)^{3+}$ ions and $(Fe, V)(3,4)^{3+}$ sites of the chains. Such an arrangement well infers that the chains are expected to display a quasi-one-dimensional magnetic structure. It is now clearly established (21) that 1D antiferromagnets display low Néel temperatues and magnetic moments (i.e., hyperfine fields at ^{57}Fe) significantly reduced by about 30% by comparing to 3-D systems, as illustrated in different crystalline pentafluorides (22–26). Indeed, the hyperfine

TABLE 4
Hyperfine Parameters in the Paramagnetic State

T (K)	IS (mm/s) ± 0.02	Γ (mm/s) ± 0.02	SQ (mm/s) ± 0.02	2ε (mm/s) ± 0.02	H_{hyp} (T) ± 0.5	% ± 2
300	0.43	0.29	1.23	—	—	29
	0.44	0.43	0.46	—	—	71
77	0.54	0.29	1.23	—	—	37
	0.53	0.36	0.44	—	—	63

Note. IS, isomer shift; G, linewidth at half height; SQ, quadrupolar splitting; %, ratio of each component.

fields at 0 K are ranging from 38 to 42 T. In the systems which exhibit isolated Fe^{3+} octahedra, the hyperfine fields are in the 51- to 53-T range as in [α-$Rb_2FeF_5(H_2O)$] and [α-$Cs_2FeF_5(H_2O)$] (27). The new [$Sr_2Fe_2F_{10}(H_2O)$] (28, 29), which displays both 1-D iron-based chains and isolated iron octahedra, with H_{hyp} (0 K) = 40.1 and 57.7 T, respectively, provides nice support to our assignement of the external sextet to Fe(1, 2) sites.

The high value of H_{hyp} of Fe(1, 2) sites is consistent with the presence of pseudoisolated octahedra weakly coupled with those of the chains. Its absorption area remains close to 26–27%, whatever the fitting procedure. All these facts converge to the same conclusion: the Fe^{3+}/V^{3+} random distribution occurs only within the chains, and it is the noncompensation (Fe/V = 7/5 in the chain) between iron ($\mu = 5\ \mu_B$) and vanadium magnetic moments ($\mu = 2\ \mu_B$) which is at the origin of the observed ferrimagnetism since, according to the Goodenough's rules, superexchange 180° interactions are antiferromagnetic for Fe^{3+}–Fe^{3+} coupling and ferromagnetic for Fe^{3+}–V^{3+} ones.

CONCLUSION

The combined analytical, structural, and magnetic studies based on X-ray diffraction and Mössbauer spectrometry have allowed to describe a new structure type in which it is demonstrated by convergent results coming from several techniques that the cationic disorder occurs only within the chains and leads to ferrimagnetic properties.

ACKNOWLEDGMENTS

The authors are indebted to Dr. P. Bonville (CEA Saclay) for the 40-mK Mössbauer spectrum registration, Dr. M. Nogues (LMOV, Versailles) for magnetic measurements, and Dr. D. Riou (Institut Lavoisier, Versailles) for X-ray data collection.

REFERENCES

1. M. Cavellec, D. Riou, C. Ninclaus, J.-M. Grenèche, and G. Férey, *Zeolites* **17,** 250 (1996).
2. K.-H. Lii, Y.-F. Huang, V. Zima, C.-Y. Huang, H.-M. Lin, Y.-C. Jiang, F.-L. Liao, and S.-L. Wang, *Chem. Mater.* **10,** 2599 (1998); V. Zima, K.-H. Lii, N. Nguyen, and A. Ducouret, *Chem. Mater.* **10,** 1914 (1998).
3. Z. A. D. Lethbridge, P. Lightfoot, R. E. Morris, D. S. Wragg, P. A. Wright, A. Kvick, and G. Vaughan, *J. Solid State Chem.* 1998, in press.
4. M. Cavellec, D. Riou, J.-M. Grenèche, and G. Férey, *J. Magn. Magn. Mat.* **163,** 173 (1996).
5. M. Cavellec, C. Egger, J. Linares, M. Nogues, F. Varret, and G. Férey, *J. Solid State Chem.* **134,** 349 (1997).
6. M. Cavellec, D. Riou, J.-M. Grenèche, and G. Férey, *M.R.S. Series* **431,** 57 (1996).
7. M. Cavellec, D. Riou, J.-M. Grenèche, and G. Férey, *Microporous Mater.* **8,** 103 (1997).
8. M. Cavellec, J.-M. Grenèche, and G. Férey, *Micro. Mesoporous Mater.* **20,** 45 (1998).
9. L. A. Meyer and R. C. Haushalter, *Inorg. Chem.* **32,** 1579 (1993).
10. R. C. Haushalter, V. Soghomonian, Q. Chen, and J. Zubieta, *J. Solid State Chem.* **105,** 512 (1993).
11. D. Whang, N. H. Hur, and K. Kim, *Inorg. Chem.* **34,** 3363 (1995).
12. M. Roca, M. D. Marcos, P. Amoros, A. Beltran-Porter, A. J. Edwards, and D. Beltran-Porter, *Inorg. Chem.* **35,** 5613 (1996).
13. J. J. Lu, Y. Xu, N. K. Goh, and L. S. Chia, *Chem. Commun.* 1710 (1998).
14. G. M. Sheldrick, SHELXTL, Univ. of Göttingen, Germany.
15. N. E. Brese and M. O'Keefe, *Acta Crystallogr.* **B47,** 192 (1991).
16. J. Teillet and F. Varret, Program MOSFIT, unpublished.
17. I. Tordjmann, R. Masse, and J. C. Guitel, *Zeit. Kristallogr.* **139,** 103 (1974).
18. T. Loiseau, P. Lacorre, Y. Calage, and G. Férey, *J. Solid State Chem.* **111,** 390 (1994).
19. M. Cavellec, D. Riou, J. M. Grenèche, and G. Férey, *Inorg. Chem.* **36,** 2187 (1997).
20. R. D. Shannon, *Acta Crystallogr.* **A32**, 751 (1996).
21. C. E. Johnson, *in* "Mössbauer Spectroscopy Applied to Inorganic Chemistry" (G. Long, Ed.), Vol. 1, p. 619. Plenum, New York.
22. G. P. Gupta, D. P. E. Dickson, and C. E. Johnson, *J. Phys. C: Solid State Phys.* **11,** 215 (1978).
23. G. P. Gupta, D. P. E. Dickson, C. E. Johnson, and B. M. Wanklyn, *J. Phys. C: Solid State Phys.* **11,** 3889 (1978).
24. G. P. Gupta, D. P. E. Dickson, and C. E. Johnson, *J. Phys. C: Solid State Phys.* **13,** 2071 (1980).
25. Y. Calage, M. C. Moron, J. L. Fourquet, and F. Palacio, *J. Magn. Magn. Mat.* **98,** 79 (1991).
26. J. L. Fourquet, R. de Pape, J. Teillet, F. Varret, and G. C. Papaefthymiou, *J. Magn. Magn. Mat.* **27,** 209 (1982).
27. Y. Calage and W. M. Reiff, *J. Solid State Chem.* **111,** 294 (1994).
28. J. M. Le Meins, Ph.D. thesis, Univ. of Le Mans, 1998.
29. J. M. Le Meins, G. Courbion, P. Bonville, W. Wernsdorfer, and J. M. Greneche, submitted.